

*The aging effect on the enhancement of thermal stability, mechanical stiffness and fluorescence properties of histidine-appended naphthalenediimide based two-component hydrogels*

Article

Accepted Version

Gayen, K., Nandi, N., Das, K. S., Hermida-Merino, D., Hamley, I. W. ORCID: <https://orcid.org/0000-0002-4549-0926> and Banerjee, A. ORCID: <https://orcid.org/0000-0002-1309-921X> (2020) The aging effect on the enhancement of thermal stability, mechanical stiffness and fluorescence properties of histidine-appended naphthalenediimide based two-component hydrogels. *Soft Matter*, 16 (44). pp. 10106-10114. ISSN 1744-683X doi: <https://doi.org/10.1039/D0SM00468E> Available at <https://centaur.reading.ac.uk/94440/>

It is advisable to refer to the publisher's version if you intend to cite from the work. See [Guidance on citing](#).

Published version at: <http://dx.doi.org/10.1039/d0sm00468e>

To link to this article DOI: <http://dx.doi.org/10.1039/D0SM00468E>

Publisher: Royal Society of Chemistry

including copyright law. Copyright and IPR is retained by the creators or other copyright holders. Terms and conditions for use of this material are defined in the [End User Agreement](#).

[www.reading.ac.uk/centaur](http://www.reading.ac.uk/centaur)

## **CentAUR**

Central Archive at the University of Reading

Reading's research outputs online

# Aging effect on the enhancement of thermal stability, mechanical stiffness and fluorescence property of a peptide appended naphthalenediimide based two component hydrogel

Kousik Gayen<sup>†</sup>, Nibedita Nandi<sup>†</sup>, Krishna Sundar Das<sup>#</sup>, xxxxxxxx, Ian W. Hamley<sup>‡</sup>, Arindam Banerjee<sup>†\*</sup>

<sup>†</sup> School of Biological Sciences, Indian Association for the Cultivation of Science, Jadavpur, Kolkata, 700032, India, Email: bcab@iacs.res.in

<sup>#</sup>School of Chemical Sciences, Indian Association for the Cultivation of Science, Jadavpur, Kolkata, 700032, India

<sup>‡</sup>Department of Chemistry, University of Reading, Whiteknights, Reading, RG6, 6AD, UK

## ABSTRACT

A dipeptide attached naphthalenediimide (NDI) containing amphiphilic molecule (NDIP) has been found to form an aggregate in aqueous solution at pH 6.6. High resolution transmittance electron microscopic (HR-TEM) analysis reveals a nice hollow nanotubular structure in the aggregated state. This peptide appended NDI forms a two component hydrogel in presence of tartaric acid in molar ratio 1:2. The morphological transformation was observed from nanotubular structure in the non-gel aggregated state of peptide appended NDI to interconnected cross-linked

nanofibers of the two component hydrogel in presence of tartaric acid. The gel was fully characterized using various techniques including wide angle powder X-ray diffraction (WAXRD), small angle X-ray scattering (SAXS), rheology, UV-vis and fluorescence spectroscopy. UV-vis study clearly indicates the J-type assembly in the aggregated state of the two component gel. Interestingly, the gel exhibits an unusual behavior upon aging compared to the fresh gel. It is found that the thermal stability and gel stiffness increase very significantly upon aging. The gel melting temperature ( $T_{gel}$ ) and storage modulus ( $G'$ ) for the fresh gel are 52°C and 32.73 rad/sec at 0.1% strain and these two parameters upon aging over 40 days are increased to 82°C and 4516.82 rad/sec respectively. Another important feature is noticed that very weakly-fluorescent nature of the fresh gel is transformed to a bright greenish fluorescent with respect to time. This result suggests that intermolecular interaction among the gelator molecules and tartaric acid in the gel phase slowly increases with time to form a mechanically very stiff and thermally robust gel. This study holds a promise for making new soft functional materials with tunable mechanical, thermal and fluorescence properties in future.

## INTRODUCTION

The design of small organic molecule based soft functional materials has gained a considerable attention to the scientists due to their wide spread application in chemistry, biology and material science<sup>1-4</sup>. Low molecular weight gels comprising of an amino acid or a peptide moiety are good building blocks for making supramolecular smart materials. Biocompatibility and biodegradable nature of these materials reinforced their usability in various research field including drug delivery<sup>5-8</sup>, tissue engineering<sup>9,10</sup>, waste water management<sup>11,12</sup>, catalysis<sup>13-15</sup>, biosensors<sup>16-17</sup> and others<sup>18-22</sup>. The gelator molecules are self-assembled by using various non-covalent interactions including hydrogen bonding interactions,  $\pi$ - $\pi$  interactions, van der Waals interaction

and others to form an entangled three dimensional network structure with lot of void spaces occupied by many solvent molecules under a suitable condition to form gels. In some cases the single gelator molecule alone is unable to form a gel. However, in presence of an additive <sup>23,24</sup> (metal ion, organic molecule) or co-assembly of two different types of gelator molecules <sup>25,26</sup> can promote gelation. This kind of gel formation is termed as two component gelation<sup>27,28</sup>. The gel property of the two component system can be regulated by varying composition and it provides better smart materials compared to a single component gel. For the last two decades, many attempts have been made to design and construct various gelator molecule with structural diversity through by the covalent attachment with naphthyl <sup>29,30</sup>, pyrene <sup>31,32</sup>, carbazole <sup>33</sup>, cholic acid<sup>34,35</sup>, sugar<sup>36-38</sup> and other groups to the lead gelator molecule. Recently, naphthalenediimides (NDI) based functional materials have become very attractive not only due to their easy synthesis, solubility, redox active nature, chemically robust, molecular planarity,  $\pi$ -acidity and n-type semiconducting nature but also due to the potential application in photovoltaic device<sup>39,40</sup>, field effect transistor<sup>41,42</sup>, solar cell<sup>43,44</sup>, sensing<sup>45-48</sup> and others <sup>49-52</sup>. However, low quantum yield restricts their application in the monomeric state of the imide substituted NDI. However, in the aggregated state, these types of molecules exhibit a significant fluorescent property owing to the aggregation induced emission (AIE) phenomenon. Various research groups have studied structure-function relationship of the gel formation, photo physical property, self-assembly/gelation, and potential application of NDI based soft functional materials in organic solvents <sup>53-55</sup>. However, there are very few reports on the self-assembly of naphthalenediimide conjugated peptide/amino acid derivative in aqueous medium <sup>56,57</sup>. This is because it is extremely difficult to dissolve the NDI based molecule in water due to the presence of bulky hydrophobic naphthyl ring. The NDI based hydrogel can be obtained by incorporating of polar group within

the NDI moiety or increasing polarity of the gelling solvent. Amino acid/peptide conjugated naphthalenediimides are able to form various fluorescent hydrogels with interesting applications<sup>58,59</sup>.

Generally the gels are studied and characterized without mentioning whether the gel is freshly prepared or aged. Sometimes the physical appearance of a gel does not change significantly upon aging. There were a few reports regarding small molecular hydrogels that describe a change in physical appearance from transparent to turbid or vice versa upon aging<sup>60-62</sup>. Adams and coworkers have reported unusual property of a dipeptide based hydrogel upon aging and over time it shows phase transfer from a freshly prepared turbid gel to a transparent aged gel<sup>63</sup>. As the time proceeds the rearrangement of the gelator molecules occur within the gel phase to form a stable network structure and the fiber -fiber interaction becomes stronger in the aged gel that leads to higher mechanical strength. If ordered arrangement of the gelator molecule is taking place within the gel phase sometimes it produced thermodynamically more stable state (crystal state)<sup>64-66</sup>. The example includes the observation of Hao and coworkers regarding the formation of fine crystallized nanospheres on the surface of a two component hydrogel nanofibers upon aging after a week<sup>67</sup>.

In course of our investigation to study the self-assembly of peptide appended naphthalenediimide NDIP, it is found that the compound NDIP (Figure 1a) forms non gel aggregate in milli-Q water at pH 6.6. However, it forms a transparent gel in presence of tartaric acid with the transformation of morphological nanotubular structure to a cross linked nanofibrous structure. Interestingly, the thermal stability, mechanical stiffness and fluorescent property can be regulated upon aging. Moreover, transparent nature of hydrogel is slowly decreases day by day to form an opaque gel after 30 days.

## EXPERIMENTAL SECTION

### Materials and Methods

11-aminoundecanoic acid, 1,4,5,8 -Naphthalenetetracarboxylic dianhydride were purchased from Aldrich. L-histidine, HOBt (1-hydroxybenzotriazole), DCC (N, N'-Dicyclohexylcarbodiimide), L-tartaric acid were purchased from SRL, India. Instrumentation details and spectroscopic analysis are given in the Supporting Information.

## RESULTS AND DISCUSSION

### Gelation Study:

Histidine containing naphthalenediimide based molecule **NDIP** has synthesized, purified and studied for gelation aqueous solution pH 6.6. It is very hard to dissolve the molecule NDIP in aqueous solution due to bulky hydrophobic naphthyl unit. The compound forms an insoluble aggregate by itself in milli-Q water. From the chemical structure it was seen that two imidazole ring was present at terminal position of the molecule. The solubility of the molecule in aqueous medium is increased in presence of a COOH containing molecule, due to acid –base interaction of COOH group and the imidazole ring of the histidine. In this context, various diacids including tartaric acid, succinic acid, malonic acid, citric acid were used for the gelation study. The co-assembly of NDIP and tartaric acid provides a stable hydrogel at particular molar ratio 1:2 (Figure 1). However, other acids are unable to form a hydrogel under the similar condition and other tested conditions attempted by using this study. For the gelation test, 12 mg (0.0128 mmol) of NDIP was taken in a glass vial and 950µL milli-Q, tartaric acid (0.0256 mmol) was added to the vial. Then the mixture was dissolved carefully by heating on a hot plate. A transparent clear

solution was observed which upon standing for 20 minutes formed a transparent stable two-component hydrogel. To get the exact molar ratio of gelator molecule and tartaric acid for a stable hydrogel, the gelation study was performed by varying the molar ratio of tartaric acid keeping the fixed gelator concentration under the similar condition. It was seen that a viscous suspension found to form when the molar ratio of NDIP and tartaric acid is 1:1. However, a clear transparent solution was found above the ratio 1:3 (NDIP: tartaric acid). It was also noticed that the gels were very weak in nature when the molar ratio is 1:1.5 or 1:2.5. So, the most stable hydrogel was obtained by co assembly of NDIP and tartaric acid at molar ratio of 1:2 and it is thermoreversible in nature. The minimum gelation concentration (MGC) was found to be 0.4 % (w/v) with respect to NDIP. The gel melting temperature ( $T_{gel}$ ) was 52°C for the freshly prepared hydrogel at 12.80 mM concentration. An interesting feature is noticed that the gel exhibits an unusual aging effect by increasing the gel melting temperature with time. The physical appearance of the gel changes as the time progresses from transparent to translucent and the gel becomes tight and rigid upon aging. Five different sets of gels were prepared under similar condition at 1:2 ratio of gelator to tartaric acid and the gel melting temperature ( $T_{gel}$ ) was measured at a fixed particular interval of time 10 day. Interestingly, it was found that  $T_{gel}$  gradually increases over the period of time (Figure S1). For the freshly prepared hydrogel the  $T_{gel}$  was 52°C whereas it becomes 82°C after 40 days. The entire study of gel melting temperature ( $T_{gel}$ ) with the progress of time is mentioned in the table 1.



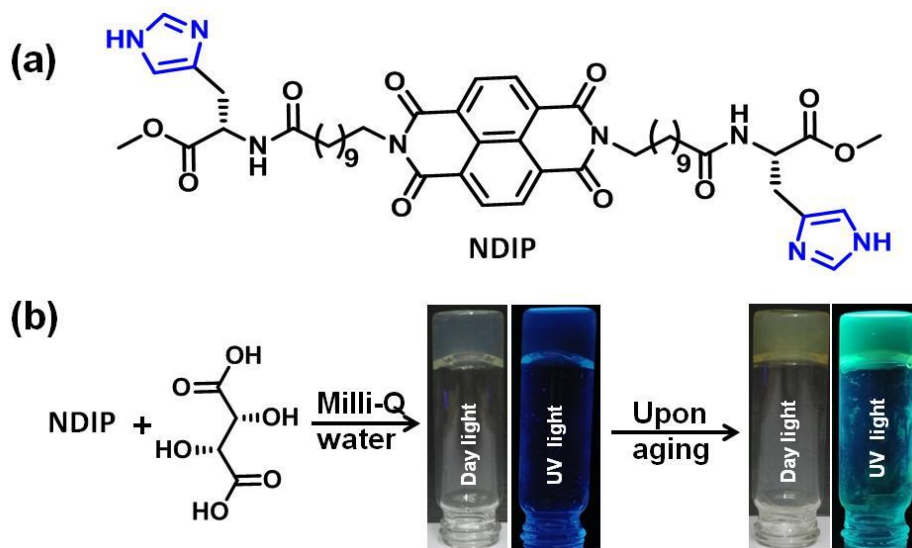


**Figure 1:** (a) Chemical structure of the gelator molecule NDIP. (b) NDIP and tartaric acid based two component hydrogel. Vial image shows the change of visual appearance and fluorescence property of gel upon aging.

### Morphological study:

High resolution transmittance electron microscopic (HR-TEM) studies were performed for insoluble aggregates of NDIP in milli-Q water as well as in the gel phase in presence of tartaric acid with a molar ratio (1:2) at different time interval (freshly prepared gel and aged gel). From the HR-TEM analysis ([Figure 2](#)) it is evident that NDIP forms holo nanotubular structure with an internal diameter 20-30 nm and total diameter 45-55 nm. However there is a sharp morphological change was observed from nanotubular structure in the aggregated non gel state to gel state of NDIP in presence of tartaric acid. The freshly prepared gel forms a cross linked nano fibrillar network structure. These nanofibers are several micrometers in length and width of the nanofiber is within the range 15-30 nm. No significant morphological change is observed of the

two component hydrogel with aging from fresh gel to aged gel. It is interesting to note that the gel formation triggered cross-linked nanofiber morphology, whereas aggregation of NDIP and succinic acid retains nanotubular morphology. The inner diameter and total diameter of the tube is 20-25 nm and 40-45 nm. Moreover in presence of citric acid the compound forms entangled nanofibrillar image with average width of the fiber 30-35 nm (Figure 2).

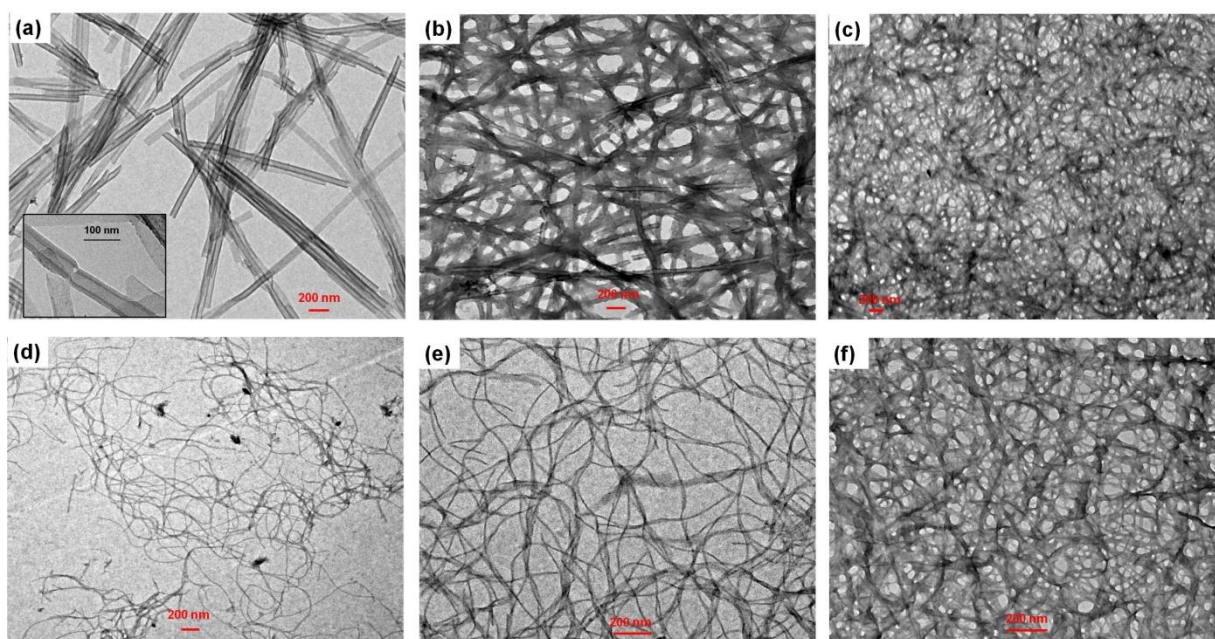


**Figure 2:** HR-TEM image of (a) aggregated state of NDIP in milli-Q water. (b) NDIP and succinic acid based aggregates (c) NDIP and citric acid based aggregates. HR-TEM image of NDIP and tartaric acid based two component gel (d) freshly prepared (e) after 10 days (f) after 40 days.

### Fourier Transform Infrared (FT-IR) Analysis:

Fourier transform infrared spectroscopic (FT-IR) study was carried out to obtain information about the non-covalent interactions among the gelator molecules within the self-assembled network structure. The significant peak appeared at 1736, 1707, 1666, 1581 $\text{cm}^{-1}$  for the compound NDIP (Figure S2). The peak corresponding to 1736, 1707, 1666  $\text{cm}^{-1}$  is due to C=O stretching frequency of the ester group of peptide, NDI moiety and amide bond of peptide unit respectively. The peak at 1581 $\text{cm}^{-1}$  indicates N-H bending of the peptide backbone. However, a noticeable FT-IR spectral change was observed for the two component hydrogel. For the freshly prepared gel or aged gel the peak originates at the position 3321 $\text{cm}^{-1}$  that can be assigned for hydrogen bonded N-H stretching of the peptide unit. A broad peak appeared in the range 3400-3600  $\text{cm}^{-1}$  can be assign to the carboxylic OH stretching frequency and alcoholic O-H of the tartaric acid. Due to the gel formation in presence of tartaric acid the peptide C=O stretching frequency of NDIP is appeared 10  $\text{cm}^{-1}$  less than that of NDIP alone in the non gel aggregated state. This indicates involvement of peptide C=O in hydrogen bonding in the gel state. A broad peak appeared at 1970  $\text{cm}^{-1}$  due to the interaction of imidazole ring of NDIP and carboxylic acid of tartaric acid<sup>26</sup>. So it can be stated that the gelation occurs due to the acid-base type of interaction involving the imidazolium N-H of NDIP and carboxylate C-O of tartaric acid (Figure S3).

### Powder X-ray Diffraction (PXRD) Studies:

To gain more information about the structural arrangement of the gelator molecules in the aggregated state wide- angle powder X-ray diffraction (WPXRD) studies were performed for the xerogel of NDIP and tartaric acid based two component hydrogel. ChemBioDraw 3D software

provides the molecular length (D) of NDIP and that is 42.77Å. In the wide angle region significant peak appeared at  $2\theta=11.61^\circ$  ( $d=7.41$  Å),  $2\theta=13.61^\circ$  ( $d=6.33$  Å),  $2\theta=17.25^\circ$  ( $d=5.01$  Å) (Figure S4) can be assign to D/6, D/7, D/8. This type WPXRD data clearly suggests the lamellar packing arrangement of the molecule NDIP in the aggregated state in aqueous medium at pH 6.6. The peaks at  $2\theta=8.10^\circ$  ( $d=10.62$ Å),  $2\theta=19.65^\circ$  ( $d=4.39$ Å) are due to the intersheet and interstrand distance of a antiparallel  $\beta$ -sheet like structure in the aggregated state of NDIP<sup>68</sup>. The peak corresponding to  $\pi$ - $\pi$  distance of imidazole ring and naphthyl unit of NDIP appeared at  $2\theta=21.22^\circ$  ( $d=4.07$  Å) and  $2\theta=21.70^\circ$  ( $d=3.98$  Å) respectively. However, a change in molecular packing arrangement for the two component gel formation and it is evident from respective WPXRD data (Figure S5). There is no significant difference of the packing pattern between fresh gel and 40 days aged hydrogel. Interestingly, there is no signature of either lamellar packing or  $\beta$ -sheet type arrangement for the two component hydrogel. The peak position of  $\pi$ - $\pi$  stacking distance of imidazole ring and naphthyl unit within the hydrogel state is more or less same and it is appeared at  $2\theta=20.54^\circ$  ( $d=3.60$  Å),  $2\theta=26.31^\circ$  ( $d=3.29$  Å) and  $2\theta=23.91^\circ$  ( $d=3.62$  Å),  $2\theta=26.53^\circ$  ( $d=3.27$  Å) for freshly prepared and 40 days aged hydrogel.

### **Small-Angle X-ray Scattering (SAXS) Study:**

To evaluate total molecular length for the interaction NDIP and tartaric acid in the gel state, small-angle X-ray scattering (SAXS) experiment was carried out. The individual molecular length obtained from ChemBioDraw 3D software for NDIP and tartaric acid is 42.77Å and 6.25Å respectively. The peak corresponding to  $d=52.33$ Å was appear in the SAXS spectra (Figure S6). The experimental value is well matched with the combine molecular length (49.02) Å of NDIP and tartaric acid. A probable model has been drawn for co-assembly of NDIP and tartaric acid in aqueous medium based on FT-IR, WPXRD, SAXS studies (Figure 5)

## Rheological study

Rheological experiment was performed to investigate the mechanical strength of the NDI based two component hydrogel at different time intervals (Figure 3) to examine whether the possibility of stiffness changes with time or not. From the frequency sweep experiment at a constant strain about 0.1 %, it is found that storage modulus  $G'$  is almost invariant over the frequency range and the storage modulus  $G'$  is always greater than loss modulus throughout the experiment. Interestingly, it was observed that storage modulus steadily increases with time from 32.73 pa for the freshly prepared gel to 4516.82 pa for the 40 days aged gel. It is evident from the table 1 that the gel stiffness is increased enormously from freshly prepared gel to 40 days aged gel. The  $G'$  value of the hydrogel is increased (146 times) upon aging after 40 days at a fixed angular frequency for the same composition of the two component gel.

**Table 1: Showing the variation of gel melting temperature, storage and loss moduli of the hydrogels at different time intervals starting from the freshly prepared gel keeping the gelator concentration same.**

Aging of gel (Day)	Gel melting temperature ( $T_{gel}$ )(°C)	Storage modulus ( $G'$ ) at an angular frequency 0.1 rad/sec	Loss modulus ( $G''$ ) at an angular frequency 0.1 rad/sec
Fresh gel	52°C	32.73	4.13
Aged after 10 days	63°C	146.56	19.84
Aged after 20 days	73°C	459.12	51.47
Aged after 30 days	79°C	1082.44	124.14

Aged after 40 days	82°C	4516.82	353.45
--------------------	------	---------	--------

Step strain experiment was carried out to investigate the thixotropic behavior of the tartaric acid based two component hydrogel (Figure S7). Different cycles for this experiment were performed starting with initial strain 0.1%. After 131 second the strain was increased to 30% to rupture the gel and it is transformed to sol. There is a crossover between  $G'$  and  $G''$  and  $G''$  is more than  $G'$  in the sol state at a fixed strain of 30% up to 256 second. After that this strain was released and it is coming back of initial strain 0.1%. To check the reproducibility of the process, the experiment is repeated for four times. Figure S8 shows that the gel can be broken upon mechanical shaking and reformed resting after 30 minutes.

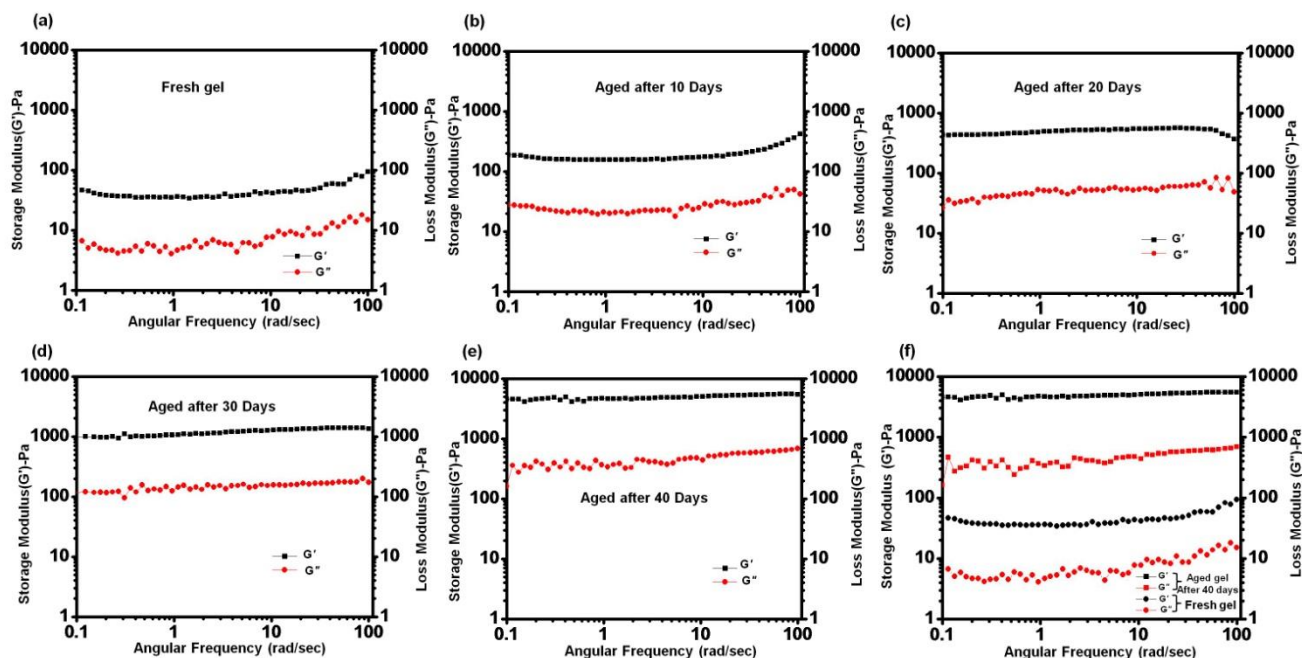


**Figure 3:** Frequency sweep experiment of NDIP and tartaric acid based two component hydrogel at a constant strain 0.1% (a) freshly prepared and after (b) 10 days (c) 20 days (d) 30 days (e) 40 days (f) combine data of freshly prepared and 40 days aged hydrogel.

### UV-Vis Study

UV-vis spectroscopic study was carried out to examine the self-assembled packing pattern of the chromophoric moiety of NDIP in monomeric state as well as in the aggregated state in presence of an organic acid (tartaric acid/succinic acid/citric acid/malic acid/malonic acid) at a fixed concentration of 0.05mM with respect to NDIP. In the monomeric state of NDIP in hexafluoroisopropanol (HFIP), sharp absorption peaks are appeared at the position 341nm, 361 nm and 381 nm. These are the characteristic peak of NDI chromophoric moiety (Figure 4). A change in self-assembly was noticed in milli-Q water for the NDIP in presence of organic acid. From the UV spectra (Figure 4) it is seen that the peak positions are appeared at 368 nm, 389 nm for the NDIP in presence of tartaric acid. These peaks are red shifted by 8 nm with a gradual decrease in intensity from the corresponding peaks in monomeric state. This observation clearly indicates a J-type self-assembly among the chromophore of NDIP in presence of tartaric acid. However, no such difference is noticed in UV spectra for the freshgel and 40 days aged gel. It is worth to mention that the self-assembled behavior of NDIP in presence of other organic acid (Figure S9) remains same as for the tartaric based two component hydrogel.



## Fluorescence study

To gain more knowledge about the aggregation behavior of the compound in presence of various organic acid fluorescence studies was carried out. The fluorescence property originates due to aggregation induced emission phenomenon of the imide substituted naphthalenediimides. We measured the fluorescence property with a finite time interval for the compound NDIP alone or in presence of organic acid in milli-Q water to examine whether the compound can show any aging effect or not. In the fluorescence spectra of aggregated NDIP in milli-Q water a sharp peak is appeared at 415 nm upon excitation at 360nm. Five different sets of aggregated solution of NDIP was prepared with finite time interval (10 day) starting from day 1. However, no such change in fluorescence spectral position or visual discrimination of these solutions (Figure 4d and Figure S10) is noticed. So, it can be said that aggregated solution of NDIP alone does not exhibit aging effect. Similarly, five set of hydrogel were prepared by NDIP and tartaric acid in such a way that age of these gels are freshly prepared, 10 days, 20 days , 30 days and 40 days aged. The physical appearance of the first two gels (freshly prepared gel and 10 days old gel) is transparent, but the transparency decreases from 20 days and after 30 days the gel becomes fully turbid (Figure 6a). The freshly prepared hydrogel does not exhibit any fluorescence property when it is seen in presence of hand held UV light ( $\lambda_{\text{max}}$  365 nm). Interestingly, it is observed that the non fluorescent gel becomes weakly greenish fluorescent aged after 20 days. The fluorescence intensity gradually increases and it emits a bright greenish fluorescence after 30 days (Figure 6c). The fluorescence spectra (Figure 4b) show that the peak appears at 465 nm upon excitation at 360 nm. Same kind of time dependent fluorescence study was performed for the non gel aggregates of NDIP and succinic acid to make it confirm whether greenish fluorescence originates due to gelation or interaction between dicarboxylic acid and imidazole



ring of NDIP in the aggregated state. Moreover, aggregate solution of succinic acid and NDIP exhibit the aging effect on the enhancement of fluorescence property (Figure 6b and 6d). Spectroscopic study show that the peak appears at 416 nm for freshly prepared aggregates of succinic acid and NDIP. As the time progress the peak position at 416 nm is started to decrease and a new peak is appeared at 465nm that becomes more prominent with time and as a result bright greenish fluorescence originate (Figure 4c). Fluorescence study convincingly demonstrates that the compound NDIP is unable to show aging effect without the presence of tartaric acid for the enhancement of fluorescence. However the combination of dicarboxylic acid and NDIP forming aggregates or gel, exhibits the enhancement of the greenish fluorescence upon aging.

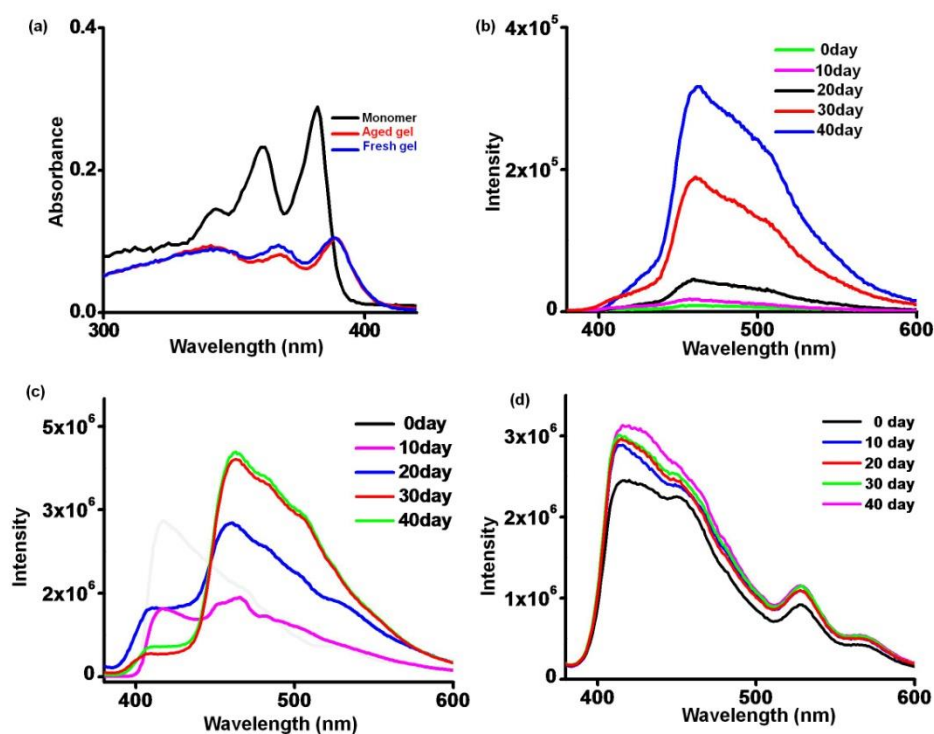


**Figure 4:** (a) UV-Vis spectra of NDIP in presence of tartaric acid (freshly prepared and 40 days aged gel). Fluorescence spectra of (b) NDIP and tartaric acid based two component hydrogel starting from fresh gel to 40 days aged gel, (c) NDIP and succinic acid based aggregates, (d) NDIP in the aggregated state in milli-Q water.

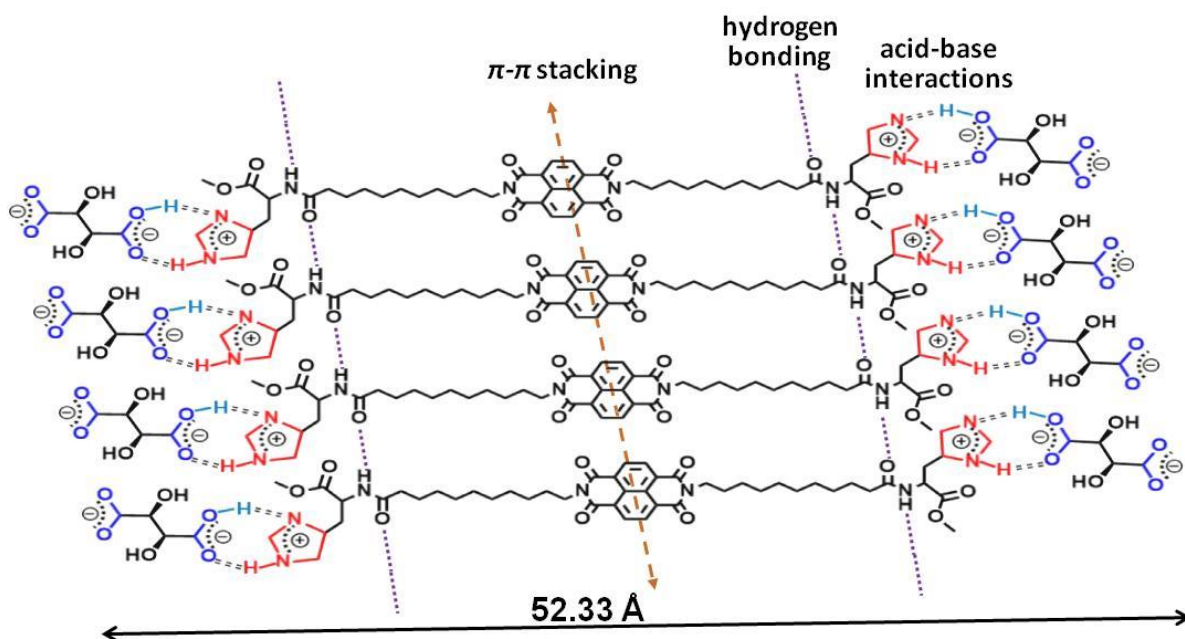


**Figure 5:** Probable packing model for NDIP and tartaric acid based two component self-assembled system in aqueous medium and — — — — lines indicate hydrogen bonding.

### Time-correlated Single Photon Counting (TCSPC) study

Time-correlated single photon counting experiment was performed to evaluate the fluorescence life time in the excited state and the decay profile for the tartaric acid based two component hydrogel in its freshly prepared form and after 40 days (aged gel). The excitation monochromator was set at 340 nm and emission was recorded at 465 nm for both gels (freshly prepared and aged). The freshly prepared hydrogel showed a bi-exponential decay profile with an average life time of 91.6 ps. Similar decay profile was observed for the aged hydrogel (after

40 days) with considerably larger average life time of 209 ps compared to the fresh hydrogel (Figure S11). So, we can conclude that excited state complex of aged gel is more stable than freshly prepared hydrogel. From the Figure 6c it is evident that the fluorescence intensity gradually increases with time for the tartaric acid based two component hydrogel. The enhancement of fluorescence promotes us to investigate whether the aging effect can influence the quantum yield of the hydrogel or not. The quantum yield was calculated by using quinine sulphate as a reference dye. Interestingly, it is observed that the quantum yield ( $\Phi$ ) of the 40 days aged hydrogel ( $\Phi = 16.19\%$ ) is much higher than that of freshly prepared hydrogel ( $\Phi = 1\%$ ). It is worth to be mentioned that succinic acid is unable to form hydrogel with NDIP. However, fluorescence intensity gradually increases for the succinic acid containing aggregates with time. Similar result of quantum yield was obtained for the freshly prepared aggregate of succinic acid and NDIP ( $\Phi = 1\%$ ). Interestingly, the quantum yield obtained from 40 days aged aggregates of succinic acid is less than that of the 40 days aged hydrogel obtained from tartaric acid and NDIP.

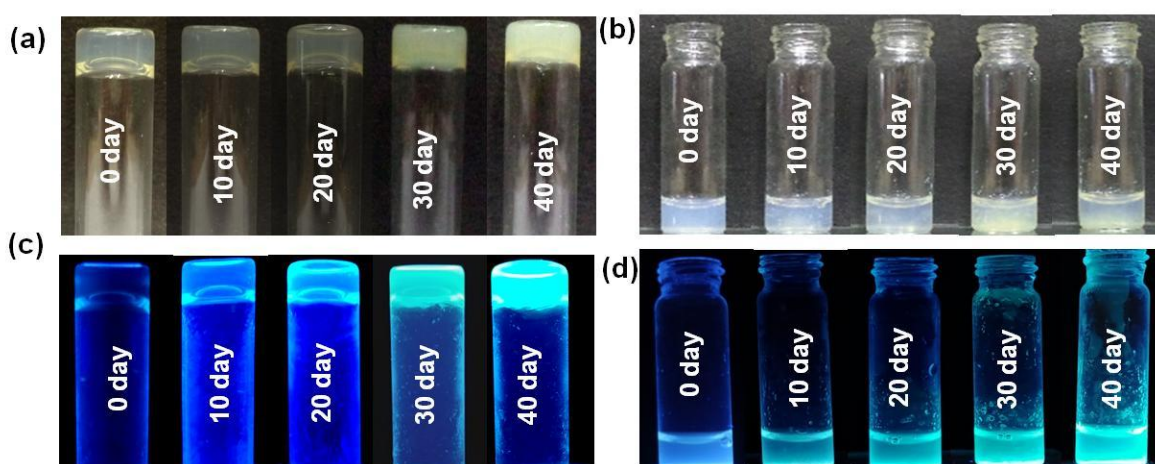


**Figure 6:** (a) The change of visual appearance and (c) enhancement of fluorescence intensity of NDIP and tartaric acid based two component hydrogel with respect to time from freshly made

gels to 40 days aged gel. (b) The change of visual appearance and (d) enhancement of fluorescence intensity of NDIP and succinic acid based two component aggregate with respect to time.

The peptide appended naphthalenediimide (NDIP) contain two terminally located imidazole rings, each having a lone pair of  $SP^2$  nitrogen atom that can act as a lewis base. Our previous report indicated that the non fluorescent xerogel film obtained from NDIP emits a bright cyan color in presence of volatile organic/inorganic acid vapors and this fluorescence was disappeared in presence of an ammonia vapors. This is an example of acid induced aggregation that leads to aggregation induced emission property. In this study in aqueous medium (milli-Q water pH 6.6) the fluorescence peak appeared at 407 nm due to the aggregation induced emission of the molecule NDIP (Figure 7). Upon the addition of TFA (trifluoroacetic acid) to the aggregated solution of NDIP, causes a sharp change in fluorescence (cyan) was observed under the UV lamp ( $\lambda_{max}=365nm$ ). The spectroscopic study indicates a peak centered at 482 nm in presence of acid whereas it appeared at 407 nm without any acid under similar condition. The strong fluorescence appeared due to the acid induced aggregation in milli-Q water. The addition of ammonia to the acidic aggregating solution causes complete loss of fluorescence (Figure 7). Due to the high dissociation constant of trifluoroacetic acid ( $3.0 \times 10^{-1}$ ) the imidazole ring protonated very fast and there is a quick appear of cyan fluorescence.

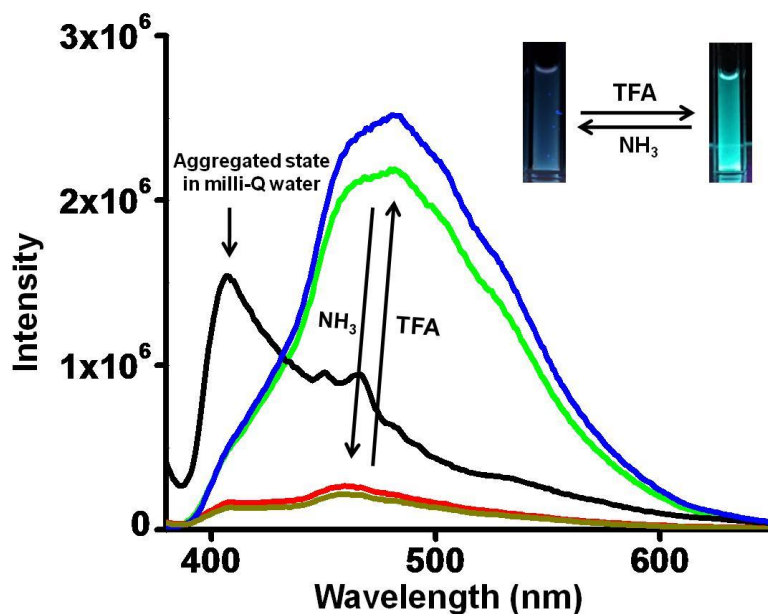


**Figure 7:** Reversible fluorescence spectra (inset: visual image of fluorescence in under UV light  $\lambda_{\text{max}}=365\text{nm}$ ) of NDIP in presence of trifluoroacetic acid (TFA) and ammonia ( $\text{NH}_3$ ).

If a weak organic dicarboxylic acid (tartaric acid or succinic acid or citric acid) is used in place of a strong acid, the NDIP is unable to form a clear solution in the presence of any of these dicarboxylic acids (tartaric acid, succinic acid, citric acid) in milli-Q water. However, it was early mentioned that NDIP forms a two-component hydrogel in the presence of tartaric acid, while succinic acid triggered a viscous solution. Due to the weak dissociation constant of those dicarboxylic acids ( $6.8 \times 10^{-4}$  for tartaric acid), the imidazole ring of the NDIP is protonated very slowly in the gel phase. As a result, the acid-induced fluorescence property of the NDIP increases very slowly in the gel state. With time, the acid-base interaction between the imidazolium ring of NDIP and the carboxylate group of tartaric acid gradually increases. As a result

the gel becomes more tight and rigid. Consequently, the gel melting temperature and mechanical stiffness gradually increases day by day from fresh gel to aged gel. Previous studies indicated that gel stiffness increases enormously due to acid-base interaction involving carboxylic acid containing peptide gelator and melamine<sup>69</sup>. The Figure 8 demonstrates that the appearance of the freshly prepared gel is very soft that is loosely held from the spatula. On the contrary, the aged gel is very rigid and tight in nature so that this gel was taken out from a vial, the sliced gel portion can be hold by a spatula, as shown in Figure 8b. Moreover, the gel is sufficiently strong and this can be cut/sliced into two prominent parts by a spatula and can be hold by a twizer (Figure 8c). The Figure 8d shows the pictorial images of the stiff sliced portion of the aged gel held by a spatula on broad daylight and under the UV-light ( excitation at 365 nm), respectively.

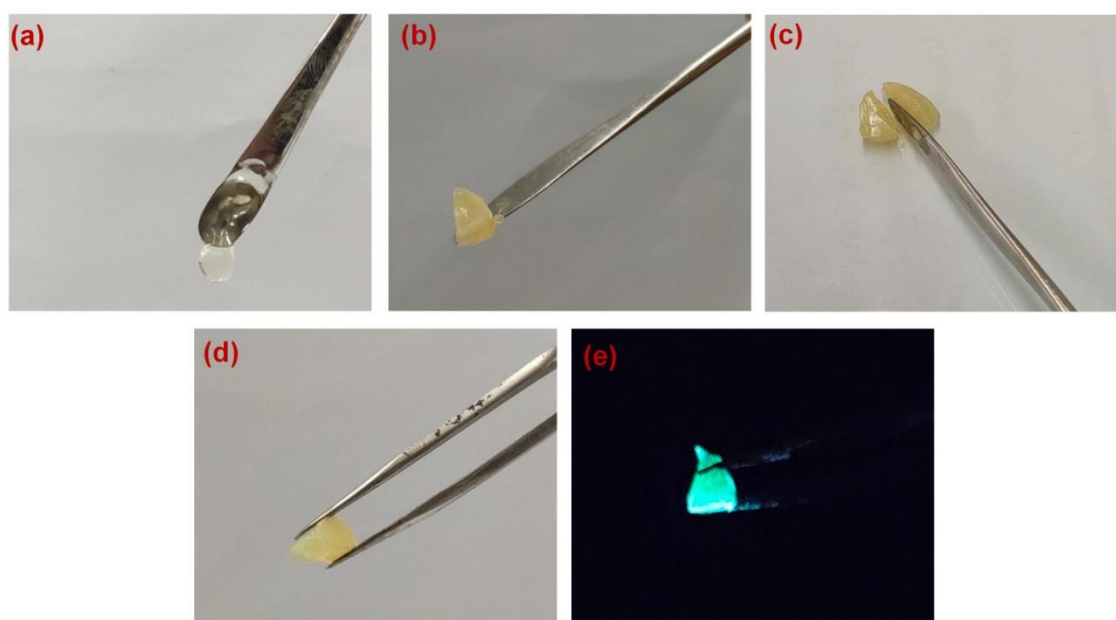


**Figure 8:** Photograph of gel with aging. (a) Showing the softness of the freshly prepared gel. (b) Image showing 40 days aged hydrogel (c) The 40 days aged hydrogel can be cut into two pieces. (d) showing the hardness of the gel taken in a twizer without deformation of the gel. (e) viewing a piece of gel in UV light.

## Conclusion

This is a wonderful example of aging effect relating to the increment of thermal stability, mechanical stiffness and fluorescence property of a peptide attached naphthalenediimide containing two component gel in presence of tartaric acid. Though there is no significant difference of morphology of the freshly prepared gel and 40 days aged gel, a clear cut morphological transformation occurs from a nanotubular structure in the aggregated state to inter connected nanofibrillar network in the gel state. The kinetics for the improvement of those properties is very slow due to the weak dissociation constant of tartaric acid. As a result the imidazole ring of the gelator molecule is slowly protonated with time and the interaction between acid and base involving carboxylate group of the tartaric acid and imidazolium unit of gelator molecule becomes prominent with time. This study indicates the tuning of thermal and mechanical stability of the two component hydrogel just by increasing time not through mixing any additive to the gel. It holds a future promise to make NDI containing peptide based tunable soft materials.

The authors declare no competing financial interest.

## Acknowledgements

K.G. and K.S.D. gratefully acknowledges CSIR, New Delhi and DST India for financial assistance respectively. N.N acknowledges IACS, India. The authors acknowledge Department of Science and Technology (DST-SERB) (DST-SERB project number: EMR/2016/005318), New Delhi for the grant. IWH acknowledges .....

## References

1. Du, X.; Zhou, J.; Shi, J.; Xu, B. Supramolecular Hydrogelators and Hydrogels : From Soft Matter to Molecular Biomaterials. *Chem. Rev.* **2015**, *115*, 13165–13307.
2. Li, J.; Xing, R.; Bai, S.; Yan, X. Recent advances of self-assembling peptide-based hydrogels for biomedical applications. *Soft Matter* **2019**, *15*, 1704—1715.
3. Yan, C.; Pochan, D. J.; Rheological properties of peptide-based hydrogels for biomedical and other applications. *Chem. Soc. Rev.*, **2010**, *39*, 3528–3540.
4. Steed, J. W. Supramolecular Gel Chemistry : Developments over the Last Decade. *Chem. Commun.*, **2011**, *47*, 1379–1383.
5. Altunbas, A.; Lee, S. J.; Rajasekaran, S. A.; Schneider, J. P.; Pochan, D. J. Biomaterials Encapsulation of Curcumin in Self-Assembling Peptide Hydrogels as Injectable Drug Delivery Vehicles. *Biomaterials* **2011**, *32* , 5906–5914.
6. Ischakov, R.; Adler-abramovich, L.; Buzhansky, L.; Shekhter, T.; Gazit, E. Bioorganic & Medicinal Chemistry Peptide-Based Hydrogel Nanoparticles as Effective Drug Delivery Agents. *Bioorg. Med. Chem.* **2013**, *21*, 3517–3522.
7. Li, J.; Mooney, D. J. Designing Hydrogels for Controlled Drug Delivery. *Nat. Rev. Mater.* **2016**, *1*, 16071.
8. Wang, H.; Yang, Z. Short-peptide-based molecular hydrogels: novel gelation strategies and applications for tissue engineering and drug delivery. *Nanoscale*, **2012**, *4*, 5259–5267.



9. Ryan, D. M.; Nilsson, B. L. Self-assembled amino acids and dipeptides as noncovalent hydrogels for tissue engineering. *Polym. Chem.*, **2012**, *3*, 18–33.
10. Saunders, L.; Ma, P. X. Self-Healing Supramolecular Hydrogels for Tissue Engineering Applications. *Macromol. Biosci.* **2019**, *19*, 1800313(1–11).
11. Okesola, B. O.; Smith, D. K.; Applying low-molecular weight supramolecular gelators in an environmental setting – selfassembled gels as smart materials for pollutant removal. *Chem. Soc. Rev.*, **2016**, *45*, 4226—4251.
12. J. P.; Knerr, Branco, M. C.; Nagarkar, R.; Pochan, D. J. ; Schneider, P. J. Heavy Metal Ion Hydrogelation of a Self-Assembling Peptide via Cysteiny l Chelation. *J. Mater. Chem.***2012**, *22*, 1352–1357.
13. Castelletto, V.; Edwards-gayle, C. J. C.; Hamley, I. W.; Pelin, J. N. B. D.; Alves, W. A.; Aguilar, A. M.; Seitsonen, J.; Ruokolainen, J. Self-Assembly of a Catalytically Active Lipopeptide and Its Incorporation into Cubosomes. *ACS Appl. Bio Mater.***2019**, *2*, 3639–3647.
14. Berdugo, C.; Miravet, J. F.; Escuder, B.; Substrate selective catalytic molecular hydrogels: the role of the hydrophobic effect. *Chem. Commun.* **2013**, *49*, 10608—10610.
15. Tena-solsona, M.; Nanda, J.; Díaz-oltra, S.; Chotera, A.; Ashkenasy, G.; Escuder, B. Emergent Catalytic Behavior of Self-Assembled Low Molecular Weight Peptide-Based Aggregates and Hydrogels. *Chem. Eur. J.* **2016**, *22*, 6687 – 6694.
16. Lian, M.; Chen, X.; Lu, Y.; Yang, W. Self-Assembled Peptide Hydrogel as a Smart Biointerface for Enzyme-Based Electrochemical Biosensing and Cell Monitoring. *ACS Appl. Mater. Interfaces* **2016**, *8*, 25036–25042.

17. King, P. J. S.; Saiani, A.; Bichenkova, E. V; Miller, A. F. A de Novo Self-Assembling Peptide Hydrogel Biosensor with Covalently Immobilised DNA-Recognising Motifs. *Chem. Commun.* **2016**, 52, 6697—6700.
18. Edwards-gayle, C. J. C.; Castelletto, V.; Hamley, I. W.; Barrett, G.; Greco, F.; Hermida-merino, D.; Rambo, R. P.; Seitsonen, J.; Ruokolainen, J. Self-Assembly, Antimicrobial Activity, and Membrane Interactions of Arginine-Capped Peptide Bola-Amphiphiles. *ACS Appl. Bio Mater.* **2019**, 2, 2208–2218.
19. Qi, G. Bin; Gao, Y. J.; Wang, L.; Wang, H. Self-Assembled Peptide-Based Nanomaterials for Biomedical Imaging and Therapy. *Adv. Mater.* **2018**, 30, 1703444 (1-34).
20. Gharazi, S.; Zarket, B. C.; Demella, K. C.; Raghavan, S. R. Nature-Inspired Hydrogels with Soft and Stiff Zones That Exhibit a 100-Fold Difference in Elastic Modulus. *ACS Appl. Mater. Interfaces* **2018**, 10, 34664–34673.
21. Garcia, A. M.; Kurbasic, M.; Kralj, S.; Melchionna, M.; Marchesan, S. A Biocatalytic and Thermoreversible Hydrogel from a Histidine-Containing Tripeptide. *Chem. Commun.* **2017**, 53, 8110—8113.
22. Zhang, C.; Shafi, R.; Lampel, A.; MacPherson, D.; Pappas, C. G.; Narang, V.; Wang, T.; Maldarelli, C.; Ulijn, R. V. Switchable Hydrolase Based on Reversible Formation of Supramolecular Catalytic Site Using a Self-Assembling Peptide. *Angew. Chem. Int. Ed.* **2017**, 56, 14511 –14515.

23. Gayen, K.; Basu, K.; Bairagi, D.; Castelletto, V.; Hamley, I. W.; Banerjee, A. Amino-Acid-Based Metallo-Hydrogel That Acts Like an Esterase. *ACS Appl. Bio Mater.* **2018**, *1*, 1717–1724.
24. Liu, Y.; Wang, T.; Li, Z.; Liu, M. Copper(II) ion selective and strong acid-tolerable hydrogels formed by an L-histidine ester terminated bolaamphiphile: from single molecular thick nanofibers to single-wall nanotubes. *ChemComm.* **2013**, *49*, 4767—4769.
25. Raeburn, J.; Adams, D. J.; Multicomponent Low Molecular Weight Gelators. *Chem. Commun.* **2015**, *51*, 5170--5180.
26. Chen, C.; Wang, T.; Fu, Y.; Liu, M.; trans–cis Configuration regulated supramolecular polymer gels and chirality transfer based on a bolaamphiphilic histidine and dicarboxylic acids *Chem. Commun.*, **2016**, *52*, 1381--1384.
27. He, Y.; Xu, M.; Gao, R.; Li, X.; Li, F.; Wu, X.; Xu, D.; Zeng, H.; Yuan, L. Two-Component Supramolecular Gels Derived from Amphiphilic Shape-Persistent Cyclo [ 6 ]Aramids for Specific Recognition of Native Arginine. *Angew. Chem. Int. Ed.* **2014**, *53*, 11834 –11839.
28. Jia, Y.; Zhu, X. X. Self-Healing Supramolecular Hydrogel Made of Polymers Bearing Cholic Acid and  $\beta$  -Cyclodextrin Pendants. *Chem. Mater.* **2015**, *27*, 387–393.
29. Yang, Z.; Liang, G.; Ma, M.; Gao, Y.; Xu, B. Conjugates of Naphthalene and Dipeptides Produce Molecular Hydrogelators with High Efficiency of Hydrogelation and Superhelical Nanofibers *J. Mater. Chem.* **2007**, *17*, 850–854.

30. Morris, K. L.; Chen, L.; Rodger, A.; Adams, J.; Serpell, L. C. Structural determinants in a library of low molecular weight gelators. *Soft Matter* **2015**, *11*, 1174–1181.
31. Hahma, A.; Bhat, S.; Leivo, K.; Linnanto, J.; Lahtinen, M.; Rissanen, K. Pyrene Derived Functionalized Low Molecular Weight Organic Gelators and Gels *New J. Chem.* **2008**, *32*, 1438–1448.
32. Pramanik, B.; Singha, N.; Das, D. Sol-, Gel-, and Paper-Based Detection of Picric Acid at Femtogram Level by a Short Peptide Gelator. *ACS Appl. Polym. Mater.* **2019**, *1*, 833–843.
33. Martin, A. D.; Robinson, A. B.; Thordarson, P. Biocompatible Small Peptide Super-Hydrogelators Bearing Carbazole Functionalities. *J. Mater. Chem. B*, **2015**, *3*, 2277–2280.
34. Zhang, M.; Fives, C.; Waldron, K. C.; Zhu, X. X. Self-Assembly of a Bile Acid Dimer in Aqueous Solutions: From Nanofibers to Nematic Hydrogels. *Langmuir* **2017**, *33*, 1084–1089.
35. Maity, M.; Maitra, U. Supramolecular Gels from Conjugates of Bile Acids and Amino Acids and Their Applications. *Eur. J. Org. Chem.* **2017**, 1713–1720
36. Datta, S.; Bhattacharya, S. Multifarious facets of sugar-derived molecular gels: molecular features, mechanisms of self-assembly and emerging applications. *Chem. Soc. Rev.* **2015**, *44*, 5596–5637.
37. Jadhav, S. R.; Vemula, P. K.; Kumar, R.; Raghavan, S. R.; John, G. Sugar-Derived Phase-Selective Molecular Gelators as Model Solidifiers for Oil Spills. *Angew. Chem. Int. Ed.* **2010**, *49*, 7695–7698.

38. Vidyasagar, A.; Handore, K.; Sureshan, K. M.; George, D. M. V. Soft Optical Devices from Self-Healing Gels Formed by Oil and Sugar-Based Organogelators. *Angew. Chem. Int. Ed.* **2011**, *50*, 8021–8024. 8021–8024.
39. Ahmed, E.; Ren, G.; Kim, F. S.; Hollenbeck, E. C.; Jenekhe, S. A. Design of New Electron Acceptor Materials for Organic Photovoltaics: Synthesis, Electron Transport, Photophysics, and Photovoltaic Properties of Oligothiophene-Functionalized Naphthalene Diimides. *Chem. Mater.* **2011**, *23*, 4563–4577.
40. Liu, Y.; Zhang, L.; Lee, H.; Wang, H. W.; Santala, A.; Liu, F.; Diao, Y.; Briseno, A. L.; Russell, T. P. NDI-Based Small Molecule as Promising Nonfullerene Acceptor for Solution-Processed Organic Photovoltaics. *Adv. Energy Mater.* **2015**, *5*, 1500195 (1-8).
41. Chen, Z.; Zhang, W.; Huang, J.; Gao, D.; Wei, C.; Lin, Z.; Wang, L.; Yu, G. Fluorinated Dithienylethene – Naphthalenediimide Copolymers for High-Mobility n - Channel Field-Effect Transistors. *Macromolecules* **2017**, *50*, 6098–6107.
42. Yuan, Z.; Ma, Y.; Geßner, T.; Li, M.; Chen, L.; Eustachi, M.; Weitz, R. T.; Li, C.; Müllen, K. Core-Fluorinated Naphthalene Diimides: Synthesis, Characterization, and Application in n-Type Organic Field-Effect Transistors. *Org. Lett.* **2016**, *18*, 456–459.
43. Park, K. H.; An, Y.; Jung, S.; Park, H.; Yang, C. Locking-In Optimal Nanoscale Structure Induced by Naphthalenediimide-Based Polymeric Additive Enables Efficient and Stable Inverted Polymer Solar Cells. *ACS Nano* **2017**, *11*, 7409–7415.
44. Lee, W.; Lee, C.; Yu, H.; Kim, D.; Wang, C.; Woo, H. Y.; Oh, J. H.; Kim, B. J. Side Chain Optimization of Naphthalenediimide – Bithiophene-Based Polymers to Enhance the

Electron Mobility and the Performance in All-Polymer Solar Cells. *Adv. Funct. Mater.* **2016**, *26*, 1543–1553.

45. Hughes, W.; Rananaware, A.; La, D. D.; Jones, L. A.; Bhargava, S.; Bhosale, S. V. Aza-Crown Ether-Core Substituted Naphthalene Diimide Fluorescence “Turn-on” Probe for Selective Detection of Ca<sup>2+</sup>. *Sensors Actuators, B Chem.* **2017**, *244*, 854–860.

46. Pandeewar, M.; Senanayak, S. P.; Govindaraju, T. Nanoarchitectonics of Small Molecule and DNA for Ultrasensitive Detection of Mercury. *ACS Appl. Mater. Interfaces* **2016**, *8*, 30362–30371.

47. Bhosale, S. V.; Bhosale, S. V.; Kalyankar, M. B.; Langford, S. J. A Core-Substituted Naphthalene Diimide Fluoride Sensor. *Org. Lett.* **2009**, *11*, 5418–5421.

48. Guha, S.; Saha, S. Fluoride Ion Sensing by an Anion -  $\pi$  Interaction. *J. Am. Chem. Soc.* **2010**, *132*, 17674–17677.

49. Fujisawa, K.; Beuchat, C.; Humbert-droz, M.; Wilson, A.; Wesolowski, T. A.; Mareda, J.; Sakai, N.; Matile, S. Anion- $\pi$  and Cation- $\pi$  Interactions on the Same Surface *Angew. Chem. Int. Ed.* **2014**, *53*, 1 – 5.

50. Ponnuswamy, N.; Pantoş, G. D.; Smulders, M. M. J.; Sanders, J. K. M. Thermodynamics of Supramolecular Naphthalenediimide Nanotube Formation: The Influence of Solvents, Side Chains, and Guest Templates. *J. Am. Chem. Soc.* **2012**, *134*, 566–573.

51. Suraru, S.-L.; Würthner, F.; Regioselectivity in Sequential Nucleophilic Substitution of TetrabromonaphthaleneDiimides. *J. Org. Chem.* **2013**, *78*, 5227–523852.

52. Kumar, Y.; Kumar, S.; Mandal, K.; Mukhopadhyay, P. Isolation of Tetracyano-Naphthalenediimide and Its Stable Planar Radical Anion *Angew. Chem. Int. Ed.* **2018**, *57*, 16318–16322.
53. Basak, S.; Nandi, N.; Baral, A.; Banerjee, A. Tailor-Made Design of J- or H-Aggregated Naphthalenediimide-Based Gels and Remarkable Fluorescence Turn on/off Behaviour Depending on Solvents. *Chem. Commun.* **2015**, *51*, 780–783.
54. Kar, H.; Gehrig, D. W.; Allampally, N. K.; Fern'andez, G.; Laquai, F.; Ghosh, S. Cooperative supramolecular polymerization of an amine-substituted naphthalene-diimide and its impact on excited state photophysical properties. *Chemical Science*. **2016**, *1*, 1115–1120.
55. Peebles, C.; Wight, C. D.; Iverson, B. L. Solution- and solid-state photophysical and stimuli-responsive behavior in conjugated monoalkoxynaphthalene–naphthalimide donor–acceptor. *J. Mater. Chem. C*, **2015**, *3*, 12156–12163.
56. Nelli, S. R.; Chakravarthy, R. D.; Lin, H. The Role of Amino Acids on Supramolecular Co- Assembly of Naphthalenediimide – Pyrene Based. *RSC Adv.*, **2018**, *8*, 14753–14759.
57. Dhiman, S.; Jain, A.; George, S. J. Communications Supramolecular Chemistry Hot Paper Transient Helicity : Fuel-Driven Temporal Control over Conformational Switching in a Supramolecular Polymer *Angew. Chem. Int. Ed.* **2017**, *56*, 1329–1333.
58. Nandi, N.; Basak, S.; Kirkham, S.; Hamley, I. W.; Banerjee, A. Two-Component Fluorescent-Semiconducting Hydrogel from Naphthalene Diimide-Appended Peptide with Long-

Chain Amines: Variation in Thermal and Mechanical Strengths of Gels. *Langmuir* **2016**, *32*, 13226–13233.

59. Hsu, L. H.; Hsu, S. M.; Wu, F. Y.; Liu, Y. H.; Nelli, S. R.; Yeh, M. Y.; Lin, H. C. Nanofibrous Hydrogels Self-Assembled from Naphthalene Diimide (NDI)/Amino Acid Conjugates. *RSC Adv.* **2015**, *5*, 20410–20413.

60. Baral, A.; Basak, S.; Basu, K.; Dehsorkhi, A.; Hamley, I. W.; Banerjee, A. Time-dependent gel to gel transformation of a peptide based supramolecular gelator *Soft Matter*, **2015**, *11*, 4944—4951.

61. Mallia, V. A.; Butler, P. D.; Sarkar, B.; Holman, K. T.; Weiss, R. G. Reversible Phase Transitions within Self-Assembled Fibrillar Networks of ( R ) -18- ( n -Alkylamino ) Octadecan-7-Ols in Their Carbon Tetrachloride Gels. *J. Am. Chem. Soc.* **2011**, *133*, 15045–15054.

62. Xie, H.; Ayoubi, M. A.; Lu, W.; Wang, J.; Huang, J.; Wang, W. A Unique Thermo-Induced Gel-to-Gel Transition in a PH-Sensitive Small- Molecule Hydrogel. *Sci. Rep.* **2017**, 1–6.

63. Draper, E. R.; McDonald, T. O.; Adams, D. J. A low molecular weight hydrogel with unusual gel aging. *Chem. Commun.* **2015**, *51*, 6595—6597.

64. Liyanage, W.; Brennessel, W. W.; Nilsson, B. L. Spontaneous Transition of Self-Assembled Hydrogel Fibrils into Crystalline Microtubes Enables a Rational Strategy To Stabilize the Hydrogel State. *Langmuir* **2015**, *31*, 9933–9942.

65. Moffat, J. R.; Smith, D. K. Metastable Two-Component Gel — Exploring the Gel – Crystal Interface. *Chem. Commun.* **2008**, 2248–2250.



66. Fichman, G.; Guterman, T.; Damron, J.; Adler-abramovich, L.; Schmidt, J.; Kesselman, E.; Shimon, L. J. W.; Ramamoorthy, A.; Talmon, Y.; Gazit, E. Spontaneous Structural Transition and Crystal Formation in Minimal Supramolecular Polymer Model. *Sci Adv.* **2016** *2*, 1-10.
67. Li, G.; Hu, Y.; Sui, J.; Song, A.; Hao J. Hydrogelation and Crystallization of Sodium Deoxycholate Controlled by Organic Acids. *Langmuir* **2016**, *32*, 1502-1509.
68. Naskar, J.; Palui, G.; Banerjee, A. Tetrapeptide-Based Hydrogels: For Encapsulation and Slow Release of an Anticancer Drug at Physiological pH. *J. Phys. Chem. B* **2009**, *113*, 11787–11792.
69. Miao, W.; Qin, L.; Yang, D.; Jin, X.; Liu, M. Multiple-Stimulus-Responsive Supramolecular Gels of Two Components and Dual Chiroptical Switches. *Chem. Eur. J.* **2015**, *21*, 1064 – 1072.